J. Fluid Mech. (1990), *vol.* 215, *pp.* 549–569
Printed in Great Britain

The interaction of waves with arrays of vertical circular cylinders

By C. M. LINTON AND D. V. EVANS
Department of Mathematics, University of Bristol, BS8 1TW, UK

(Received 3 August 1989)

The scattering of water waves by an array of N bottom-mounted vertical circular cylinders is solved exactly (under the assumption of linear water wave theory) using the method proposed by Spring & Monkmeyer in 1974. A major simplification to this theory has been found which makes the evaluation of quantities such as the forces on the cylinders much simpler. New formulae are given for the first and mean second-order forces together with one for the free-surface elevation in the vicinity of a particular cylinder. Comparisons are made between the exact results shown here and those generated using the approximate method of McIver & Evans (1984). The behaviour of the forces on the bodies in the long-wave limit is also examined for the special case of two cylinders with equal radii.

1. Introduction

With the construction of large ocean structures such as oil rigs which consist of a number of legs on which is mounted some form of structure, the interaction between water waves and arrays of bodies has become increasingly important and much work has been done on the subject in recent years. Most notably Kagemoto & Yue (1986) have shown how a general three-dimensional water-wave diffraction problem concerning a structure consisting of a number of separate elements can be solved exactly in terms of the diffraction characteristics of each of the individual elements. This is a powerful method which solves in principle all multiple-body diffraction problems where the solutions are already known for the individual elements.

In the present work attention is restricted to the particularly simple, but not unrealistic, geometry, of N vertical circular cylinders spanning the whole depth of water. This enables progress to be made analytically which leads to expressions for the various quantities of interest which are simple to compute. The fact that the cylinders extend throughout the depth of water allows the depth dependence to be factored out of the problem and eliminates the need to consider evanescent modes. With the depth dependence removed the problem is equivalent to the two-dimensional acoustic problem of scattering by N sound hard circular cylinders, about which much has been written.

The direct method of solution that we shall use here was devised by Záviška (1913) and rediscovered for the case of water waves by Spring & Monkmeyer (1974). Other methods of solution for this problem have been considered, notably that pioneered by Twersky (1952) who constructed a solution using an iterative procedure in which successive scatters by each of the cylinders were introduced at each order. This method was extended to the water-wave case by Ohkusu (1974). The main drawback of this iterative scheme is that it rapidly becomes unmanageable as the number of bodies increases. A brief survey of these and other methods for the solution of the

acoustic problem is given in Martin (1985). In the context of water waves Mingde & Yu (1987) have studied the case of shallow water-wave diffraction of multiple circular cylinders using the same multiple scattering techniques as Spring & Monkmeyer (1974). Much of the work on the problem of the scattering of water waves by an array of bodies has been to evaluate forces, both the amplitude and phase of the first-order force and the mean second-order drift force, since it is well known (see, for example, Molin 1979) that this drift force on a body can be calculated from the solution to the linear first-order potential problem. Both these problems will be considered here as well as the evaluation of free-surface amplitudes. This is important in the design of structures such as oil rigs where it is necessary to avoid the waves created by the interaction between the legs of the platform slamming into the underside of the upper structure. Clearly when the waves are large nonlinear effects will be very important but an analysis of the linear problem should give a good qualitative picture of the kind of resonances that the interactions between the elements of the structure are likely to produce.

In this paper it will be shown how the method of Spring & Monkmeyer (1974) can be considerably improved upon. A simplified expression for the velocity potential in the vicinity of a particular cylinder is developed which leads to simple formulae for the first- and mean second-order forces on that body and also provides an efficient method for the calculation of free-surface amplitudes.

An approximate solution to this problem based on the work of Simon (1982) was given by McIver & Evans (1984) in which they assumed that the cylinders were widely spaced. They approximated the circular waves emanating from a particular cylinder as a plane wave at the other cylinders. Comparison is made in their paper between their approximate results and those of the exact theory for the first-order force and the results show a very good agreement even when the cylinders are fairly closely spaced. Here we shall compare the values obtained for the free-surface elevations in the two cases. This is perhaps a more stringent test since the force is an integrated quantity whereas the free-surface elevation is not.

2. Formulation

Under the usual assumption of linear water wave theory there exists a velocity potential $\Phi(x, y, z, t)$, where x and y are coordinates in the mean free-surface and z is vertically upwards. We assume that there are $N (\geqslant 1)$ fixed vertical circular cylinders each of which extends from the bottom, $z = -h$, up through the free surface. The depth dependence of the problem can then be factored out and if we also assume that all motion is time harmonic with angular frequency ω we can write

$$\Phi(x, y, z, t) = \mathrm{Re}\{\phi(x, y) f(z) \, \mathrm{e}^{-\mathrm{i}\omega t}\}, \tag{2.1}$$

where

$$f(z) = -\frac{\mathrm{i}gA}{\omega} \frac{\cosh \kappa(z+h)}{\cosh \kappa h} \tag{2.2}$$

and κ is the real positive solution of the dispersion relation

$$\kappa \tanh \kappa h = K \equiv \omega^2/g. \tag{2.3}$$

The free-surface elevation is then given by

$$H(x, y, t) = \mathrm{Re}\{\eta(x, y) \, \mathrm{e}^{-\mathrm{i}\omega t}\}, \tag{2.4}$$

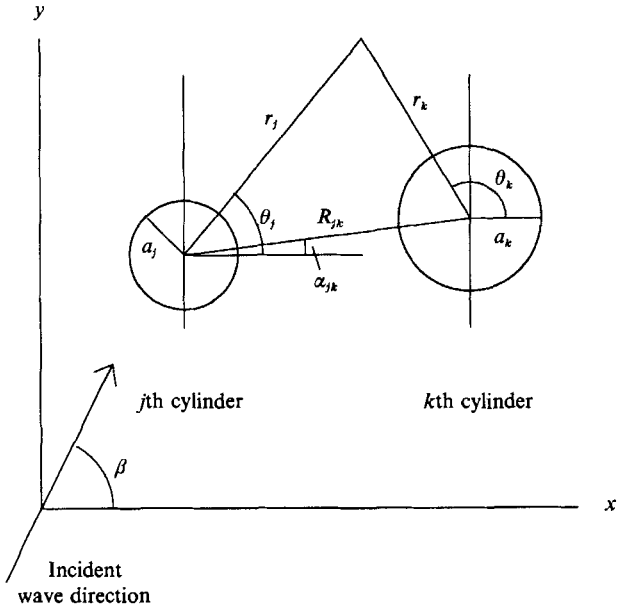

FIGURE 1. Plan view of two cylinders.

where
$$\eta(x, y) = A\phi(x, y). \tag{2.5}$$

Thus A represents the amplitude of the incident wave.

We will use $N+1$ coordinate systems: (r, θ) are polar coordinates in the (x, y)-plane centred at the origin whilst (r_j, θ_j), $j = 1, \ldots, N$ are polar coordinates centred at (x_j, y_j) which is the centre of the jth cylinder. The various parameters relating to the relative positions and sizes of the N cylinders are shown in figure 1.

An incident plane wave making an angle β with the x-axis is characterized by

$$\begin{aligned}\phi_{\mathrm{I}} &= \mathrm{e}^{\mathrm{i}\kappa(x\cos\beta + y\sin\beta)} \equiv \mathrm{e}^{\mathrm{i}\kappa r\cos(\theta-\beta)} \\ &= I_j \mathrm{e}^{\mathrm{i}\kappa r_j\cos(\theta_j-\beta)},\end{aligned} \tag{2.6}$$

where $I_j (= \mathrm{e}^{\mathrm{i}\kappa(x_j\cos\beta + y_j\sin\beta)})$ is a phase factor associated with cylinder j. This in turn can be written

$$\phi_{\mathrm{I}} = I_j \sum_{n=-\infty}^{\infty} J_n(\kappa r_j)\,\mathrm{e}^{\mathrm{i}n(\pi/2-\theta_j+\beta)}; \tag{2.7}$$

see, for example, Gradshteyn & Ryzhik (1965, p. 973, equation M027).

Now the effect of a given cylinder on the incident wave will be to produce a scattered wave which will in turn be scattered by adjacent cylinders and so on. A description of all the possible interactions that take place is provided by associating with each cylinder a general wave potential describing waves radiating away from that cylinder, which, together with the incident wave potential, describes the total wave field.

A general form for such a radiating wave emanating from cylinder j is

$$\phi_{\mathrm{s}}^j = \sum_{n=-\infty}^{\infty} A_n^j Z_n^j H_n(\kappa r_j)\,\mathrm{e}^{\mathrm{i}n\theta_j} \tag{2.8}$$

for some set of complex numbers A_n^j. Here

$$Z_n^j (\equiv Z_{-n}^j) = J_n'(\kappa a_j)/H_n'(\kappa a_j), \quad H_n(\kappa r_j) \equiv J_n(\kappa r_j) + \mathrm{i}Y_n(\kappa r_j).$$

The introduction of the factor Z_n^j simplifies the results that will be obtained. If, instead of $A_n^j Z_n^j$, we put B_n^j in (2.8) then it can be shown that $J_n'(\kappa a_j) = 0$ implies $B_n^j = 0$ and so no restrictions are being added by the inclusion of the factor Z_n^j. Clearly the value of A_n^j is irrelevant if $J_n'(\kappa a_j) = 0$ and so we shall assume that this is not the case in the following analysis. The total potential can thus be written

$$\phi = \phi_1 + \sum_{j=1}^{N} \phi_s^j$$

$$= \mathrm{e}^{\mathrm{i}\kappa r\cos(\theta-\beta)} + \sum_{j=1}^{N}\sum_{n=-\infty}^{\infty} A_n^j Z_n^j H_n(\kappa r_j)\,\mathrm{e}^{\mathrm{i}n\theta_j}. \tag{2.9}$$

Using Graf's addition theorem for Bessel functions (Gradshteyn & Ryzhik 1965, p. 979, equation WA394(6)) we can express (2.9) in terms of the coordinates (r_k, θ_k) and then apply the boundary conditions which are

$$\frac{\partial\phi}{\partial r_k} = 0 \quad \text{on} \quad r_k = a_k, \quad k = 1,\ldots,N. \tag{2.10}$$

Some algebra leads to the following infinite systems of equations:

$$A_m^k + \sum_{\substack{j=1\\ \neq k}}^{N}\sum_{n=-\infty}^{\infty} A_n^j Z_n^j \mathrm{e}^{\mathrm{i}(n-m)\alpha_{jk}} H_{n-m}(\kappa R_{jk}) = -I_k \mathrm{e}^{\mathrm{i}m(\pi/2-\beta)},$$

$$k = 1,\ldots,N, \quad -\infty < m < \infty. \tag{2.11}$$

It is important to note that in using the addition theorem for Bessel functions in order to write functions of (r_j, θ_j) in terms of the coordinates (r_k, θ_k) we have had to assume that $r_k < R_{jk}$. This is certainly true on the boundary of the kth cylinder for all j and thus (2.11) is valid. The expression obtained for (r_k, θ_k) is in fact

$$\phi(r_k,\theta_k) = \sum_{n=-\infty}^{\infty} [I_k J_n(\kappa r_k)\,\mathrm{e}^{\mathrm{i}n(\pi/2-\theta_k+\beta)} + A_n^k Z_n^k H_n(\kappa r_k)\,\mathrm{e}^{\mathrm{i}n\theta_k}]$$

$$+ \sum_{\substack{j=1\\ \neq k}}^{N}\sum_{n=-\infty}^{\infty} A_n^j Z_n^j \sum_{m=-\infty}^{\infty} J_m(\kappa r_k) H_{n+m}(\kappa R_{jk})\,\mathrm{e}^{\mathrm{i}m(\pi-\theta_k)}\,\mathrm{e}^{\mathrm{i}(n+m)\alpha_{jk}} \tag{2.12}$$

and this expression is valid if $r_k < R_{jk}$ for all j. This is therefore an expansion valid near to cylinder k. Replacing m by $-m$ in the final term allows us to write this term as

$$\sum_{m=-\infty}^{\infty}\left(\sum_{\substack{j=1\\ \neq k}}^{N}\sum_{n=-\infty}^{\infty} A_n^j Z_n^j H_{n-m}(\kappa R_{jk})\,\mathrm{e}^{\mathrm{i}(n-m)\alpha_{jk}}\right) J_m(\kappa r_k)\,\mathrm{e}^{\mathrm{i}m\theta_k}.$$

The group of terms contained within the brackets can now be substituted for using the infinite system of equations (2.11). The resulting simple formula is

$$\phi(r_k,\theta_k) = \sum_{n=-\infty}^{\infty} A_n^k (Z_n^k H_n(\kappa r_k) - J_n(\kappa r_k))\,\mathrm{e}^{\mathrm{i}n\theta_k} \quad \text{if} \quad r_k < R_{jk} \quad \forall j. \tag{2.13}$$

This expression is, to the authors' knowledge, new and provides an extremely simple formula for the velocity potential near any cylinder. In particular the velocity potential on the kth cylinder reduces to

$$\phi(a_k,\theta_k) = -\frac{2\mathrm{i}}{\pi\kappa a_k}\sum_{n=-\infty}^{\infty}\frac{A_n^k}{H_n'(\kappa a_k)}\mathrm{e}^{\mathrm{i}n\theta_k}, \tag{2.14}$$

where Wronskian relations for Bessel functions have been used.

In order to evaluate the constants A_n^j the infinite system (2.11) is truncated to an $N(2M+1)$ system of equations in $N(2M+1)$ unknowns:

$$A_m^k + \sum_{\substack{j=1 \\ \neq k}}^{N} \sum_{n=-M}^{M} A_n^j Z_n^j \, \mathrm{e}^{\mathrm{i}(n-m)\alpha_{jk}} H_{n-m}(\kappa R_{jk}) = -I_k \, \mathrm{e}^{\mathrm{i}m(\pi/2-\beta)},$$

$$k = 1, \ldots, N, \quad m = -M, \ldots, M. \quad (2.15)$$

By increasing M greater accuracy can be achieved at the expense of computing time. It was found that, except when the cylinders are very close together, taking $M = 6$ produced results accurate to four significant figures and in all following calculations, unless otherwise stated, this value was used.

Note that the solution for the case $N = 1$ is given exactly by

$$A_m^1 = -I_1 \, \mathrm{e}^{\mathrm{i}m(\pi/2-\beta)} \quad (2.16)$$

and the equivalence of the expressions (2.13) and (2.9) is clear because of the incident wave expansion (2.7). If we assume that the cylinder is at the origin and $\beta = 0$ this gives

$$A_m^1 = -\mathrm{i}^m, \quad (2.17)$$

recovering the result of MacCamy & Fuchs (1954).

3. Forces

The first-order force on the jth cylinder is given by integrating the pressure over the surface of the cylinder. It is $\mathrm{Re}\{X^j \mathrm{e}^{-\mathrm{i}\omega t}\}$ where

$$X^j = -\frac{\rho g A a_j}{\kappa} \tanh \kappa h \int_0^{2\pi} \phi(a_j, \theta_j) \begin{Bmatrix} \cos\theta_j \\ \sin\theta_j \end{Bmatrix} \mathrm{d}\theta_j. \quad (3.1)$$

(The upper elements of a bracketed pair refer to the force in the x-direction and the lower elements to that in the y-direction.) Evaluation of the integral, using (2.14), gives

$$X^j = -\begin{Bmatrix} \mathrm{i} \\ 1 \end{Bmatrix} \frac{2\rho g A \tanh \kappa h}{\kappa^2 H_1'(\kappa a_j)} \left(A_{-1}^j \begin{Bmatrix} - \\ + \end{Bmatrix} A_1^j \right). \quad (3.2)$$

The time-independent factor in the first-order force on an isolated cylinder in the direction of motion, F, can be found using (2.17). We find

$$F = \frac{4\rho g A \tanh \kappa h}{\kappa^2 H_1'(\kappa a)} \quad (3.3)$$

and

$$|X^j| = \tfrac{1}{2}|F| \left| A_{-1}^j \begin{Bmatrix} - \\ + \end{Bmatrix} A_1^j \right|. \quad (3.4)$$

The amplitude of the first-order force on multiple circular cylinders has been considered by many previous authors, for example Spring & Monkmeyer (1974), and so we shall not dwell here on the results that can be obtained from (3.4). One example will be sufficient and this is shown in figure 2. Here we are concerned with four cylinders arranged at the vertices of a square of side length R. The various parameters are $a/h = 0.5$, $R/h = 2$ and $\beta = \frac{1}{4}\pi$. The cylinders are numbered clockwise 1–4 and are situated at $(-h, h)$, (h, h), $(h, -h)$ and $(-h, -h)$ respectively, so that the forces in the direction of wave advance on cylinders 1 and 3 are identical. The curve

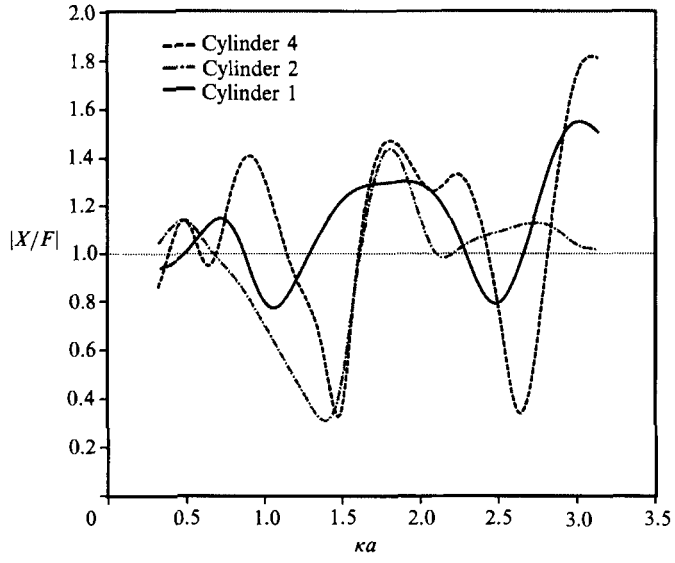

FIGURE 2. Non-dimensional amplitude of the first-order force in the direction of wave advance plotted against κa for a group of four cylinders situated at the vertices of a square ($a/h = \frac{1}{2}$, $R/h = 2, \beta = \frac{1}{4}\pi$).

shows that interaction effects can be extremely important in determining the amplitude of the first-order force.

We now turn our attention to the mean second-order drift force. The drift force is associated with a transfer of momentum by the waves and is essentially a nonlinear phenomenon. However, it has been shown that the contribution to the mean second-order drift force, as was mentioned in the introduction, can be calculated purely from the first-order potential. This force is generally small compared with the first-order force but, unlike that force, because the drift force is steady with constant magnitude, it can be very important when considering problems such as the mooring of structures.

The drift force on the jth cylinder may be written as follows:

$$f^j \equiv f^j_x + \mathrm{i} f^j_y = \alpha \int_0^{2\pi} \left\{ \frac{1}{\kappa^2} |\nabla\phi|^2 \Big|_{r_j = a_j} - |\phi|^2 \Big|_{r_j = a_j} \right\} \mathrm{e}^{\mathrm{i}\theta_j} \, \mathrm{d}\theta_j, \tag{3.5}$$

where

$$\alpha = \tfrac{1}{8}\rho g A^2 a_j \left(1 + \frac{2\kappa h}{\sinh 2\kappa h}\right)$$

(Eatock Taylor & Hung 1985). Note that this is a time-independent quantity and that the real and imaginary parts of f^j correspond to the drift force in the x- and y-directions respectively. For a detailed discussion of the complete second-order diffraction problem for an axisymmetric body, including a derivation of this expression, the reader is directed to Kim & Yue (1989).

From (2.13) it follows that

$$\nabla\phi|_{r_j = a_j} = \left(0, \frac{2}{\pi\kappa a_j^2} \sum_{n=-\infty}^{\infty} \frac{n A_n^j \mathrm{e}^{\mathrm{i}n\theta_j}}{H_n'(\kappa a_j)}\right). \tag{3.6}$$

Using this expression together with equation (2.14) gives, after some manipulation,

$$f = \frac{8\alpha}{\pi(\kappa a)^2} \sum_{n=-\infty}^{\infty} \left(\frac{n(n+1)}{(\kappa a)^2} - 1 \right) \frac{A^*_{n+1} A_n}{H'^*_{n+1}(\kappa a)\, H'_n(\kappa a)}, \tag{3.7}$$

where we have omitted the sub- and superscript js for convenience and an asterisk denotes the complex conjugate. This can be written

$$f = \frac{8\alpha}{\pi(\kappa a)^2} \sum_{n=0}^{\infty} \left(\frac{n(n+1)}{(\kappa a)^2} - 1 \right) \left(\frac{A^*_{n+1} A_n}{H'^*_{n+1}(\kappa a)\, H'_n(\kappa a)} - \frac{A^*_{-n} A_{-n-1}}{H'^*_n(\kappa a)\, H'_{n+1}(\kappa a)} \right) \tag{3.8}$$

which is a more convenient form for computation. From (2.16) we have that in the single cylinder case

$$A^*_{n+1} A_n = A^*_{-n} A_{-n-1} = -\mathrm{i}\, \mathrm{e}^{\mathrm{i}\beta}, \tag{3.9}$$

which gives, after some simplification involving Wronskian relations for Bessel functions,

$$f_1 = \frac{32\alpha}{\pi^2(\kappa a)^3} \mathrm{e}^{\mathrm{i}\beta} \sum_{n=0}^{\infty} \left(\frac{n(n+1)}{(\kappa a)^2} - 1 \right)^2 \frac{1}{|H'_n(\kappa a)|^2\, |H'_{n+1}(\kappa a)|^2}. \tag{3.10}$$

This expression is given in Appendix B of Kim & Yue (1989).

Using (3.8) and (3.10) we can compute the non-dimensional drift force in the direction of wave advance, f/f_1, for the same configuration as in figure 2 and this is shown in figure 3. Four curves are shown, one each for cylinders 1, 2 and 4 and then one which is the sum of the drift forces on all four cylinders. The curves show that, as in the case of first-order forces, interaction effects are extremely important when determining the drift force on either individual elements of a structure or on the structure as a whole. Note that for some wavenumbers the drift force on cylinder 4 is in the opposite direction to the direction of the incident wave with a magnitude greater than that of f_1.

Eatock Taylor & Hung (1985) speculated that the total drift force on a group of N identical cylinders in the direction of wave advance tends to N^2 times the drift force on an isolated cylinder as the wavenumber, κa, tends to zero (i.e. in the long-wave limit). This was subsequently proved by McIver (1987) using matched asymptotic expansions, who showed that F, the total drift force on the group non-dimensionalized with respect to the drift force on a single cylinder satisfies

$$\lim_{\kappa a \to 0} F = N^2 + O(a/R)^2, \tag{3.11}$$

where R is a typical separation between the columns. However, in his paper McIver points out that if the cylinders are placed at the vertices of a regular polygon then the second term in this expansion vanishes and we are left with

$$\lim_{\kappa a \to 0} F = N^2 + O(a/R)^4, \tag{3.12}$$

The N^2 result is shown very clearly in figure 4 which plots F against κa for three configurations; an equilateral triangle, a square and a regular pentagon. In each case the ratio of the cylinder radius to the length of the side of the regular polygon concerned was 0.05.

The behaviour of multicolumn structures in very long waves is of considerable practical importance, particularly in the case of the drift force as this is closely related to highly damped resonances that can be excited in irregular seas by sum and

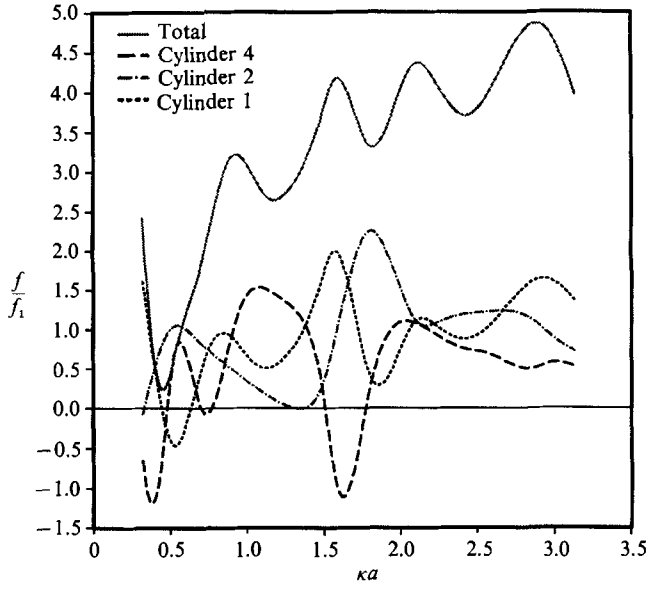

FIGURE 3. Non-dimensional drift force in the direction of wave advance plotted against κa for four cylinders arranged as in figure 2.

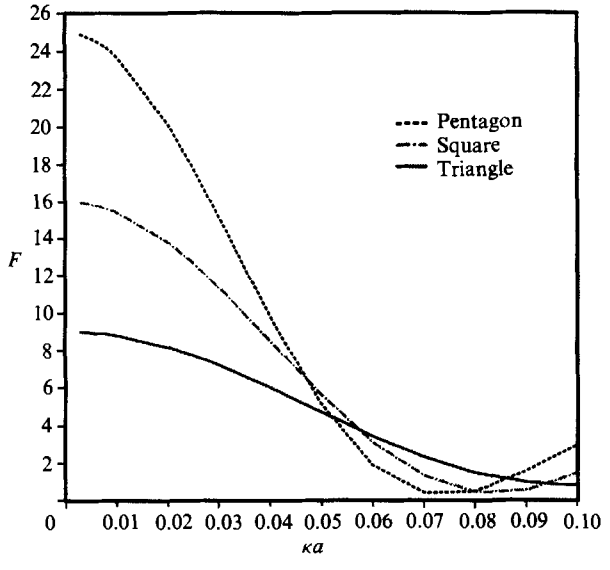

FIGURE 4. Total non-dimensional drift force on a group of cylinders plotted against κa for three configurations, all with the cylinders situated at the vertices of a regular polygon.

difference frequency effects which, owing to the low natural frequencies of certain modes of large offshore structures, can have a major influence on fatigue and thus the lifetime of such structures. In the next section we look in more detail at the behaviour of the infinite system (2.11) in the long-wave limit.

4. Long-wave approximations

Some analytic progress can be made towards the solution of (2.11) in the case of long waves. The term long waves is used to mean waves whose length is much greater than the spacing between the cylinders, i.e. the limit $\kappa a_j \to 0$ with a_j/R_{jk} fixed. An alternative limiting procedure would be $\kappa a_j \to 0$ with $\kappa R_{jk} = O(1)$ which corresponds to a 'small body' limit. This second case is not very interesting as the system of equations (2.11) simply reduces to the N single cylinder equations $A_m^k = -I_k \mathrm{e}^{\mathrm{i}m(\pi/2-\beta)}$, $k = 1, \ldots, N$. Thus the interaction effects become negligible as the ratio of the body radius to the separation becomes small, a not very surprising result.

The limit $\kappa a_j \to 0$, a_j/R_{jk} fixed is more difficult to analyse and to facilitate this analysis we shall restrict our attention to the case of two cylinders of equal radius. Without any loss of generality we can fix the relative positions of the cylinders and consider the effect of varying the incident wave angle, β. Here we will take $\alpha_{12} = -\frac{1}{2}\pi$ ($\alpha_{21} = \frac{1}{2}\pi$). The case $\beta = 0$ was considered by Eatock Taylor & Hung (1985). They assumed that the leading-order behaviour of the coefficients could be obtained, at least approximately, by considering a small truncation size. The value they used was $M = 1$. It is natural to ask what differences, if any, are obtained if a larger value of M is used. Here we shall look at the problem (for arbitrary β) with $M = 1$ and then with $M = 2$.

As $\kappa a_j \to 0$ the problem is related to that of uniform flow past the cylinders with an upstream velocity, U, given by $A(g/h)^{\frac{1}{2}}$. When $\beta = 0$ this problem is equivalent to that of uniform flow past a cylinder next to a wall and it will be instructive to look at this before studying the full problem. The geometry is as shown in figure 5 and the details can be found in Appendix A.

Thus, from (A 17), we expect to find that in the limit as $\kappa a \to 0$ with $\beta = 0$ there is a steady suction force between the cylinders of magnitude

$$2\pi a \rho g A^2 \lambda^3 (1 + 2\lambda^2) + O(\lambda^7), \tag{4.1}$$

where $\lambda = a/R_{12} (\equiv a/2b)$.

We begin by assuming that for any M the solutions of the truncated system (2.15) are approximations to the actual solutions of the full problem which would be obtained by letting $M \to \infty$. In particular it is reasonable to assume that, as $\kappa a \to 0$, the order of magnitude of the coefficients A_m^k is independent of the truncation parameter M. Now, by considering $M = 0$, and letting $\kappa a \to 0$ in (2.15) we find that $A_0^k = O(1)$ ($k = 1, 2$), and by the previous assumption this is true for all M. By examining in detail equation (2.15) with $M = 1$ and $\kappa a \to 0$, we find that $A_{\pm 1}^k = O(1)$ also ($k = 1, 2$). In order to determine these coefficients, we retain only the leading-order terms in the 6×6 matrix. We find after inversion that $A_0^k \to -1$,

$$(1 - \lambda^4) A_{\pm 1}^k = \mp \mathrm{i}(\mathrm{e}^{\mp \mathrm{i}\beta} + \lambda^2 \mathrm{e}^{\pm \mathrm{i}\beta}) \quad (k = 1, 2). \tag{4.2}$$

If we substitute these results into the formula for the first-order force, (3.4), we get

$$|X| \sim |F| \left| \begin{Bmatrix} (1 - \lambda^2)^{-1} \cos\beta \\ (1 + \lambda^2)^{-1} \sin\beta \end{Bmatrix} \right|, \tag{4.3}$$

which is an approximation to the amplitude of the exciting force as $\kappa a \to 0$ using a truncation parameter $M = 1$.

For small λ, this agrees, up to order λ^2, with the formula derived by McIver (1987) using matched asymptotic expansions and, for $\beta = 0$, with that obtained by Eatock

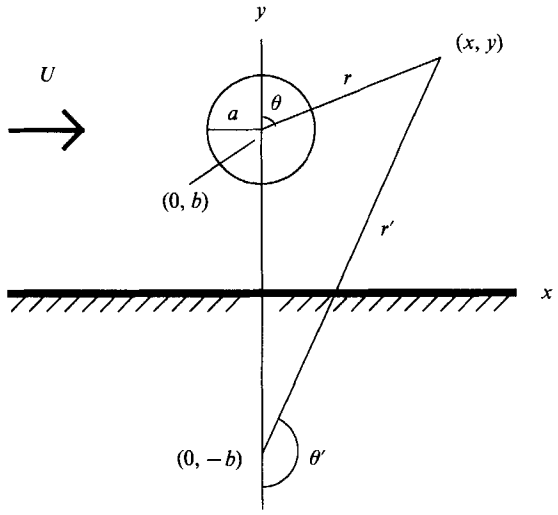

FIGURE 5. Coordinate system for uniform flow past a cylinder next to a wall.

λ	McIver (1987) $\begin{pmatrix}(1+\lambda^2)\cos\beta\\(1-\lambda^2)\sin\beta\end{pmatrix}$	Equn (4.3) $\begin{pmatrix}(1-\lambda^2)^{-1}\cos\beta\\(1+\lambda^2)^{-1}\sin\beta\end{pmatrix}$	Based on numerical computation of (2.15)
0.1	$\begin{pmatrix}0.875\\0.495\end{pmatrix}$	$\begin{pmatrix}0.875\\0.495\end{pmatrix}$	$\begin{pmatrix}0.875\\0.495\end{pmatrix}$
0.2	$\begin{pmatrix}0.901\\0.480\end{pmatrix}$	$\begin{pmatrix}0.902\\0.481\end{pmatrix}$	$\begin{pmatrix}0.902\\0.481\end{pmatrix}$
0.3	$\begin{pmatrix}0.944\\0.455\end{pmatrix}$	$\begin{pmatrix}0.952\\0.459\end{pmatrix}$	$\begin{pmatrix}0.953\\0.459\end{pmatrix}$
0.4	$\begin{pmatrix}1.005\\0.420\end{pmatrix}$	$\begin{pmatrix}1.031\\0.431\end{pmatrix}$	$\begin{pmatrix}1.046\\0.435\end{pmatrix}$

TABLE 1. First-order force magnification factor, $\beta = \frac{1}{6}\pi$

Taylor & Hung (1985). However, for arbitrary $\lambda\,(<\frac{1}{2})$ equation (4.3) gives results which are closer to those obtained from a full numerical solution of (2.15) than those which are obtained by only retaining terms up to order λ^2. The variations are shown in table 1 where it can be seen that equation (4.3) is within $< 2\%$ of the exact value even for $\lambda = 0.4$.

Next we turn to the case $M = 2$ where the analysis is not so straightforward. The details can be found in Appendix B. The following results are obtained for small λ:

$$\left.\begin{aligned} A^1_{-1} &= A^2_{-1} = \mathrm{i}[(1+\lambda^4)\,\mathrm{e}^{\mathrm{i}\beta} + \lambda^2\,\mathrm{e}^{-\mathrm{i}\beta}] + O(\lambda^6),\\ A^1_{1} &= A^2_{1} = -\mathrm{i}[\lambda^2\,\mathrm{e}^{\mathrm{i}\beta} + (1+\lambda^4)\,\mathrm{e}^{-\mathrm{i}\beta}] + O(\lambda^6),\\ A^1_{-2} &= -A^2_{-2} = -\frac{4\lambda^3}{\kappa a}[\lambda^2\,\mathrm{e}^{\mathrm{i}\beta} + \mathrm{e}^{-\mathrm{i}\beta}] + O(\lambda^6),\\ A^1_{2} &= -A^2_{2} = \frac{4\lambda^3}{\kappa a}[\mathrm{e}^{\mathrm{i}\beta} + \lambda^2\,\mathrm{e}^{-\mathrm{i}\beta}] + O(\lambda^6). \end{aligned}\right\} \tag{4.4}$$

'Exact' formulae, in terms of λ, can be calculated but without solving for $M > 2$ we cannot be confident of the accuracy of the higher-order coefficients and so these have been omitted. If we substitute these expressions into (3.4) we find

$$|X| = |F| \left| \begin{Bmatrix} (1+\lambda^2+\lambda^4)\cos\beta \\ (1-\lambda^2+\lambda^4)\sin\beta \end{Bmatrix} \right| + O(\lambda^6) \tag{4.5}$$

which is precisely the same as (4.3) when expanded in powers of λ.

This agreement for both $M = 1$ and $M = 2$ up to order λ^4 gives confidence in the validity of the result (4.5), in the long-wave limit.

Let us now turn our attention to the drift force. The drift force on a single cylinder, given by (3.10), reduces to

$$f_1 \sim \tfrac{5}{16}\rho g A^2 a\pi^2 \left(1+\frac{2\kappa h}{\sinh 2\kappa h}\right) e^{i\beta}(\kappa a)^3 \tag{4.6}$$

in the long-wave limit, where it should be noted that the first two terms in the series in (3.10) are required to obtain this leading-order behaviour. This expression is identical to that obtained by McIver (1987) using far-field considerations.

We now have sufficient information to examine the magnitude of the first two terms in the series expression (3.8) for the drift force on one cylinder in a group of two. From (3.8), and the facts that $A_0 = -1$, $A_{-1} = A_1^*$ and $A_{-2} = -A_2^*$, we obtain, for the first two terms in the expression for f,

$$f = \frac{8\alpha}{\pi}\left[-\frac{iA_1^*}{4}\pi^3(\kappa a)^3 + \frac{A_1 A_2^*}{4}\pi^2\kappa a\right]. \tag{4.7}$$

From (4.4) the first term in (4.7) is $O(\kappa a)^3$, which is the same order as f_1, but the second term is $O(1)$. Numerical observations suggest that the second term is dominant over all other terms in (3.8) but without solving (2.15) for larger values of M we are unable to prove this. Under this assumption, substituting from (4.4) gives, for small λ up to order λ^5,

$$f \sim -i\pi\rho g a A^2 \left(1+\frac{2\kappa h}{\sinh 2\kappa h}\right)\lambda^3(2\lambda^2+e^{-2i\beta}) \quad \text{as} \quad \kappa a \to 0. \tag{4.8}$$

If we assume that $a/h = O(1)$ then $\kappa h \to 0$ as $\kappa a \to 0$ and (4.8) reduces to

$$\frac{f_x}{\rho g a A^2} \sim -2\pi\lambda^3 \sin 2\beta \tag{4.9}$$

and

$$\frac{f_y}{\rho g a A^2} \sim -2\pi\lambda^3(\cos 2\beta + 2\lambda^2), \tag{4.10}$$

which is equivalent to (4.1) if $\beta = 0$.

Eatock Taylor & Hung (1985) looked at the long-wave limit of the drift force by considering just the first term in (3.8). This work shows that the second term must be considered for any valid conclusions to be drawn.

The N^2 behaviour of the total drift force is not picked up by this analysis as it is not related to the leading-order behaviour of the drift force.

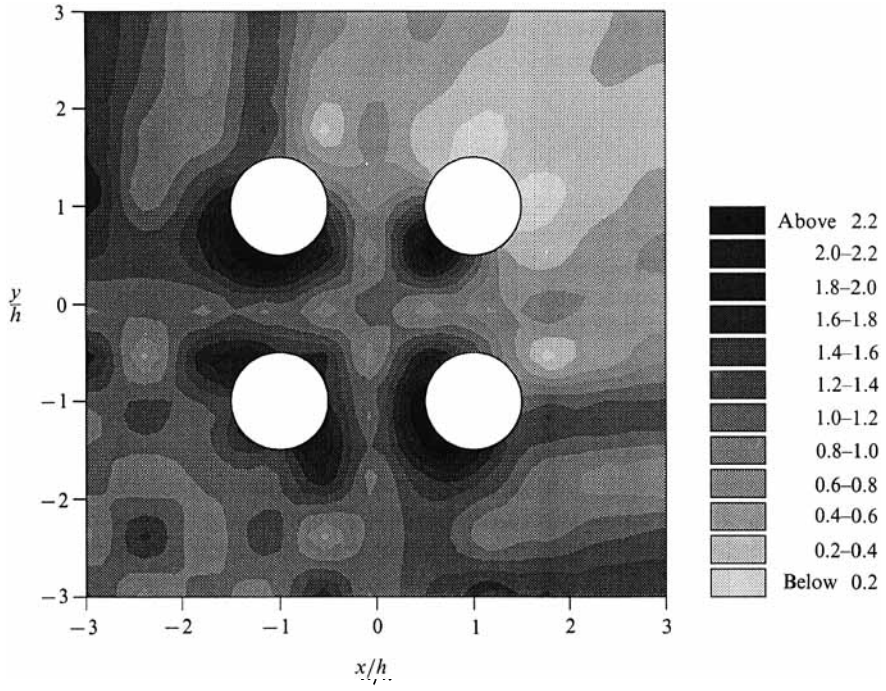

FIGURE 6. Maximum free-surface amplitudes due to the interaction of an incident plane wave ($\beta = \frac{1}{4}\pi, \kappa h = \pi$) on a group of four cylinders ($a/h = 0.5$) arranged at the vertices of a square.

5. Free-surface amplitudes

The amplitude of the free surface is given by (2.4) and thus for a unit-amplitude incident wave

$$|H(x, y, t)| = |\phi(x, y)|. \tag{5.1}$$

Equation (2.13) provides an extremely efficient method for the evaluation of free-surface amplitudes near to a particular cylinder. Because of its range of validity it can be used at most places of interest in the vicinity of some cylinder k. However, this will not be the case far from the cylinder group when (2.9) must be used.

There is an endless number of cylinder configurations which could be examined. We shall illustrate typical results by considering one or two situations having application in the offshore industry.

We begin by considering the array of cylinders in the form of a square, which was used in figures 2 and 3 in considering the forces on individual legs of an offshore drilling platform.

Thus figure 6 shows a plot of $|\phi|$ for this configuration for $\kappa a = \frac{1}{2}\pi$ corresponding to a wavelength of $\lambda = 2h$. In the absence of the cylinders the plot would be a uniform shade of grey corresponding to a relative maximum wave amplitude of unity. The incident waves in figure 6 approach from the south-west. Two features stand out: the build-up in front of cylinders 1, 2 and 3 is over twice the amplitude of the incident wave whereas in the lee of cylinder 2 destructive interference causes the free-surface amplitude to be less than 40% of that of the incident wave.

Figures 7, 8 and 9 show results for different wavelengths when an incident wave with $\beta = 0$ (from the west in the figures) is incident on the same square of cylinders as used in figure 6. The figures correspond to wavelengths of $3h$, $4h$ and $5h$

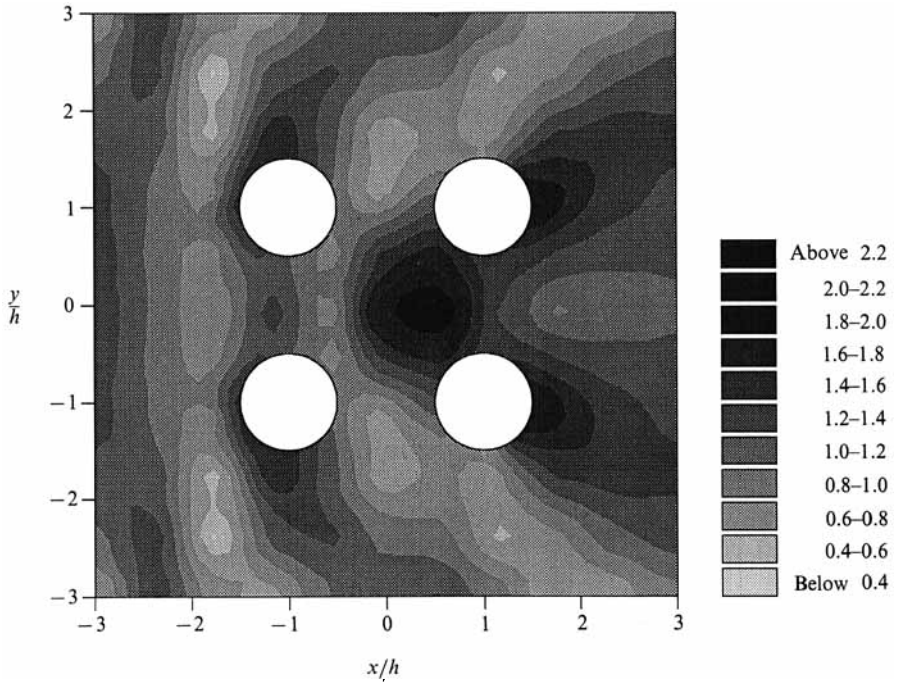

FIGURE 7. Maximum free-surface amplitudes due to the interaction of an incident plane wave ($\beta = 0, \kappa h = \frac{2}{3}\pi$) on a group of four cylinders ($a/h = 0.5$) arranged at the vertices of a square.

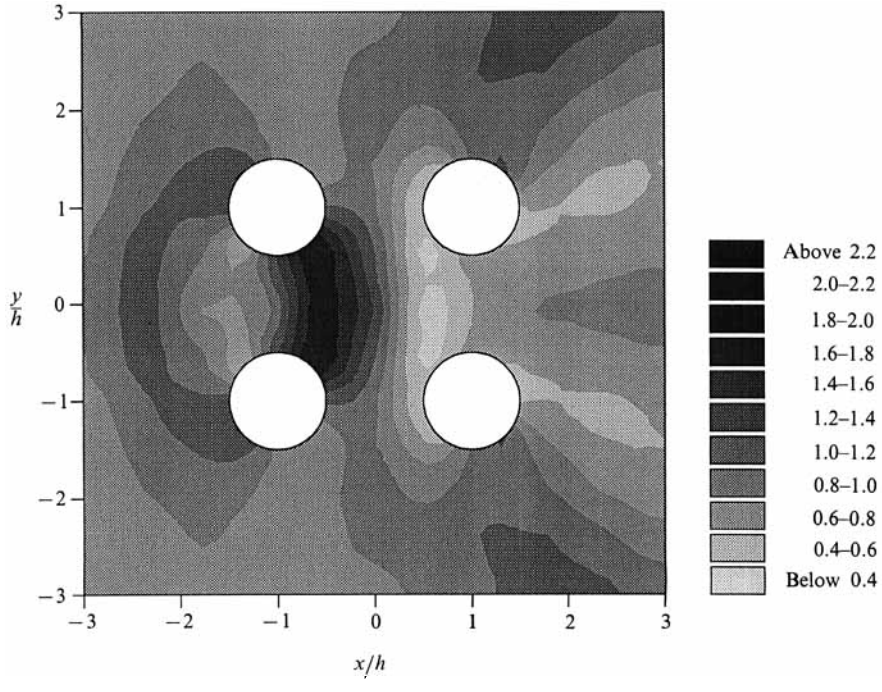

FIGURE 8. Maximum free-surface amplitudes due to the interaction of an incident plane wave ($\beta = 0, \kappa h = \frac{1}{2}\pi$) on a group of four cylinders ($a/h = 0.5$) arranged at the vertices of a square.

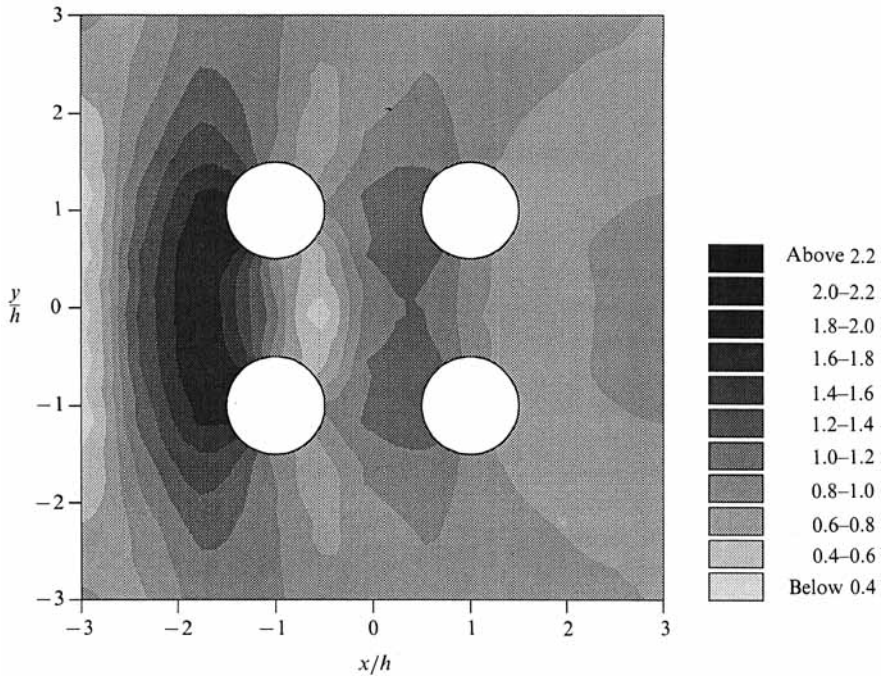

FIGURE 9. Maximum free-surface amplitudes due to the interaction of an incident plane wave ($\beta = 0, \kappa h = \frac{2}{3}\pi$) on a group of four cylinders ($a/h = 0.5$) arranged at the vertices of a square.

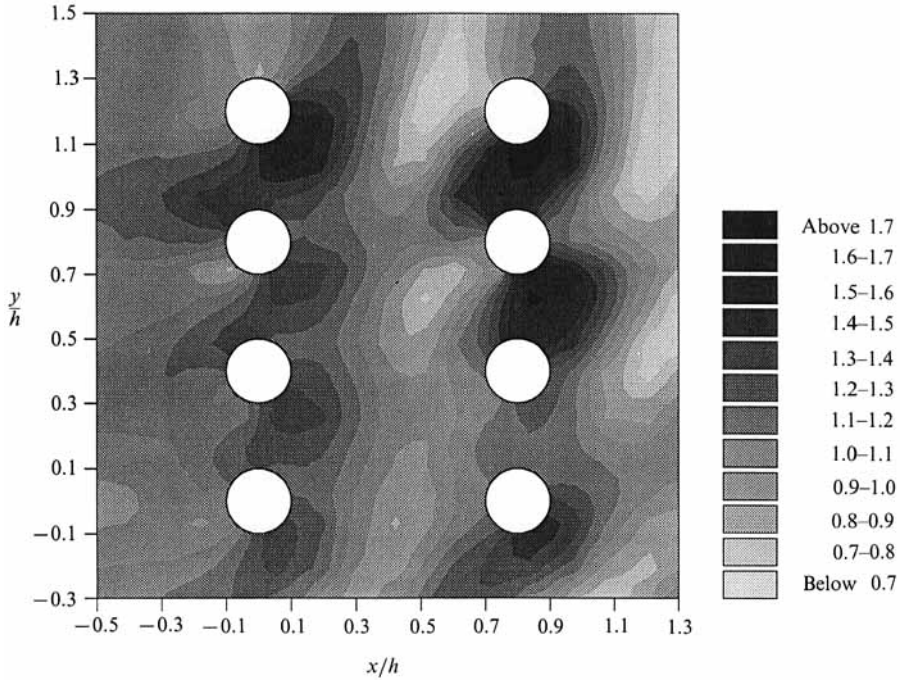

FIGURE 10. Maximum free-surface amplitudes due to the interaction of an incident plane wave ($\beta = \frac{3}{4}\pi, \kappa h = 2\pi$) on a group of eight cylinders ($a/h = 0.1$) arranged in two parallel rows of four.

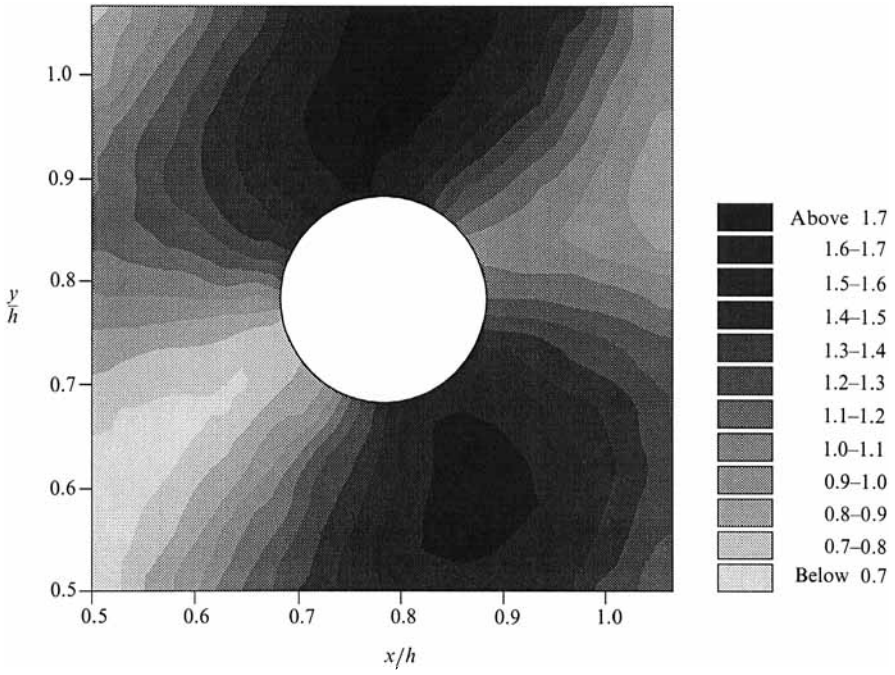

FIGURE 11. Detail of the maximum free-surface amplitude in the vicinity of the cylinder centred at $(0.8h, 0.8h)$ in figure 10.

respectively. The maximum amplitudes that result are similar for the three values of λ but the position of the large waves is crucially dependent on λ.

Cylinders arranged at the vertices of squares are typical of oil-rig-like structures and as such are interesting configurations to examine. Another structure of interest is a jetty consisting of two rows of fairly closely spaced cylinders. Figure 10 shows such a situation with two rows of four cylinders all with $a/h = 0.1$. The wavenumber κa is $\frac{1}{5}\pi$ and the incident wave angle is $\beta = \frac{3}{4}\pi$ (from the south-east in figure 10). It can be seen that there is a large build-up around the cylinder centred at $(0.8h, 0.8h)$ and this is shown in more detail in figure 11 which was obtained using the near-cylinder form (2.13). Once the system of equations (2.15) has been solved the evaluation of free-surface amplitudes from (2.13) to produce results like those shown in figure 11 is extremely straightforward and quick and is preferable to using a boundary integral or equivalent numerical scheme which has been developed for more general geometries. It should be remembered, however, that the present method is limited to the circular geometry considered here.

6. Comparison with the plane-wave approximation

McIver & Evans (1984) produced an approximate method based on the work of Simon (1982) for the solution of the N vertical cylinder problem using the idea that if the cylinders are sufficiently far apart then a wave emanating from one of the cylinders can be approximated by a plane wave when it reaches another cylinder. Comparison is made in their paper between results for the first-order force obtained from their method and results obtained from the exact method of Spring &

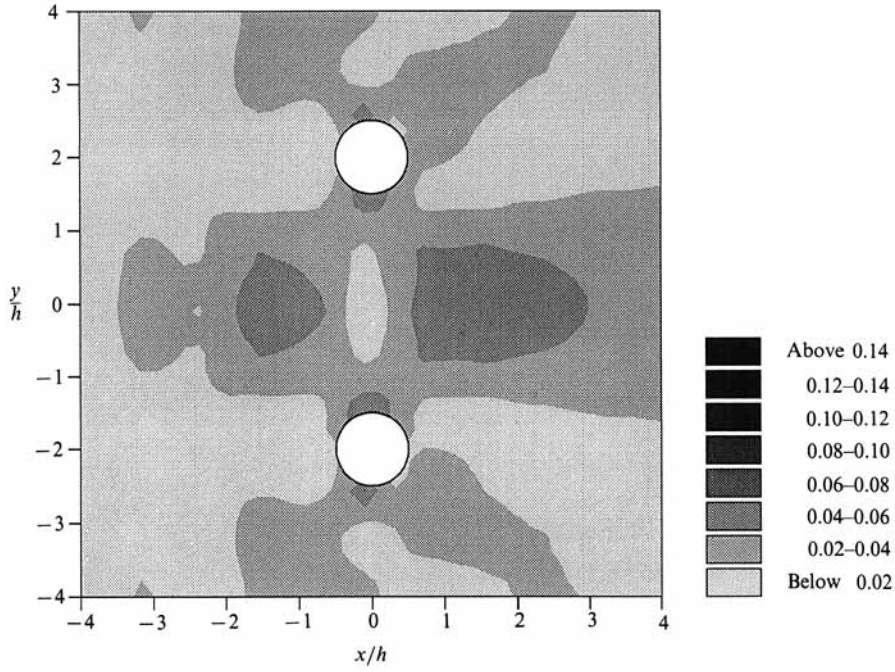

FIGURE 12. Difference in amplitudes predicted by the exact method and the plane-wave approximation when a plane wave ($\beta = 0, \kappa h = 1$) is incident on two widely spaced cylinders ($a/h = 0.5$).

Monkmeyer (1974). These comparisons show that the plane-wave approximation is remarkably good even for relatively close spacings.

It is informative to examine the relative effort that must be used to solve this problem by these two methods. In the exact formulation an $N(2M+1)$ system must be solved and typically $M \approx 6$ gives four-figure accuracy. In the approximate method an $N(N-1)$ system results and this immediately shows that for large values of N, the exact method requires the solution of a smaller system. There are other factors that determine the total time required to set up and solve these systems, and results in McIver & Evans (1984) show that for $N \leqslant 5$ and $M \geqslant 3$ the plane-wave approximation takes less time to solve, though for these small values of N neither is very time consuming. However, if one is interested in computing the free-surface elevations in the vicinity of a group of cylinders, the amount of effort required to solve the truncated system of equations (2.15) is insignificant compared to that needed to evaluate the potential at a large number of points. Such calculations are best done using the exact formulation since even without using the improved plane-wave approximation each evaluation of ϕ requires the computation of N^2 sums of the form $\sum_{n=-\infty}^{\infty} B_n H_n(\kappa r)\, e^{in\theta}$. With the new simple formula (2.13) the velocity potential in the vicinity of a particular cylinder can be obtained from one such sum, and at points where (2.13) is not available equation (2.9), which contains N such sums, must be used. These sums converge fairly rapidly but the saving from using the exact method described here can still be very significant particularly when N is large. For example in figure 11 where $N = 8$, the potential was evaluated at 400 different points on the free surface and thus 400 sums computed. To do the same calculation using the plane-wave approximation would have required the evaluation of 25600 such sums. It is therefore clear that in the problem considered in this paper, having the

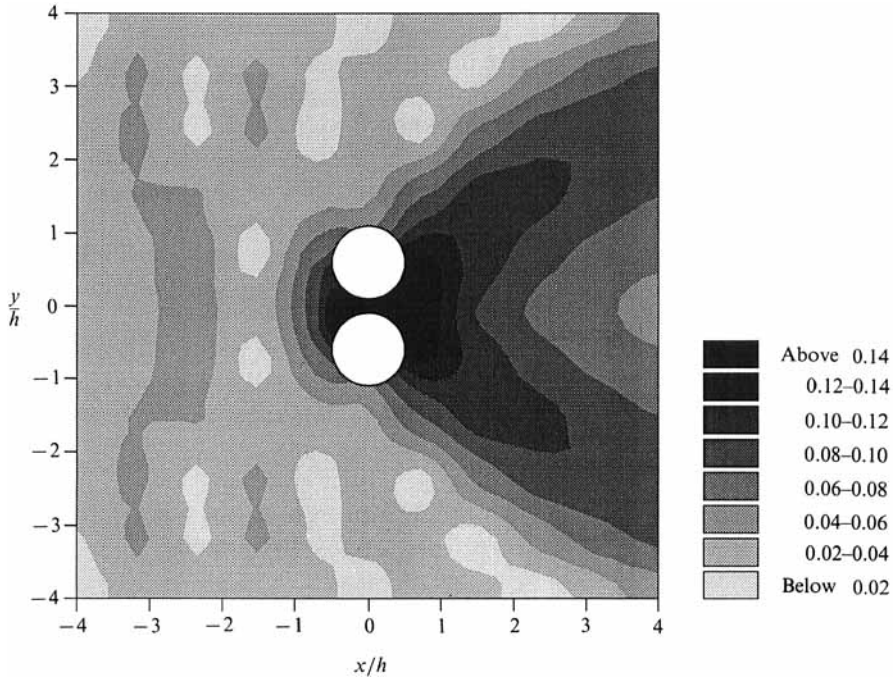

FIGURE 13. Difference in amplitudes predicted by the exact method and the plane-wave approximation when a plane wave ($\beta = 0, \kappa h = 1$) is incident on two closely spaced cylinders ($a/h = 0.5$).

particularly simple geometry of N vertical circular cylinders extending throughout the depth, it is more appropriate to use the exact method. If, however, we were interested in a multiple scattering problem that could not easily be solved exactly then the plane-wave approximation would be useful. We shall therefore use the circular cylinder problem as a test problem to explore the limitations of the method of McIver & Evans in predicting maximum wave amplitude.

Thus figures 12 and 13 show the absolute value of the difference between the maximum free-surface amplitude predicted by the approximate method and that given by the exact formulation for a wave normally incident on two cylinders. In figure 12 the separation between the centres of the cylinders is $8a$ and we can see that the maximum error is less than 6%. The cylinders are much closer together in figure 13 with the separation only $2.4a$ and the error is also greater. At its maximum the error is only about 15%, however, and considering the closeness of the cylinders and the nature of the approximation this is remarkably accurate. It should be emphasized that this is a comparison of the free-surface amplitude for the complete problem, i.e. the incident wave plus the scattered wave. The size of the differences shown using the different methods is due to two competing factors: the method being employed, and the relative magnitude of the scattered wave compared to the incident wave. Thus in situations where the cylinders have little effect on the wave field, such as in very long waves, we have found that the two methods produce very similar answers for the total wave field. This contrasts with the usual assumption for the validity of the plane-wave approximation, namely κR large, or short waves compared to cylinder spacing.

7. Conclusion

The exact theory for the scattering of waves by N vertical circular cylinders developed by Spring & Monkmeyer (1974) is exploited to make major simplifications in the calculation of forces and free-surface amplitudes. The full theory is also used to propose improved expressions for the drift force on one of two cylinders in long waves. It is shown that the method is more efficient than the approximate method of McIver & Evans (1984) when a number of cylinders, N, is large. However, their method is applicable to a wider class of problems and the high quality of their approximation has been confirmed here for the wave amplitude even for closely spaced cylinders.

Applications in the area of offshore structures are presented. The present method can also be extended to consider the effect of incident waves on an infinite row of identical equally spaced vertical cylinders and also to solve acoustic radiation problems in two-dimensions.

C.M.L. is supported by SERC (MTD Ltd.) grant no. GR/F/32226. The authors would like to thank Dr J. B. Lawrie for useful discussions.

Appendix A

One possible way to solve the problem of uniform flow past a cylinder next to a wall is to let the velocity potential be given by

$$\Phi = Ux + \psi \tag{A 1}$$

and then ψ must satisfy

$$\nabla^2\psi = 0 \quad \text{in the fluid,} \tag{A 2}$$

$$\frac{\partial\psi}{\partial y} = 0 \quad \text{on} \quad y = 0, \tag{A 3}$$

$$\frac{\partial\psi}{\partial r} = -U\sin\theta \quad \text{on} \quad r = a \tag{A 4}$$

and

$$\psi \to 0 \quad \text{as} \quad |x| \to \infty. \tag{A 5}$$

In order to determine ψ write

$$\psi = U\sum_{n=1}^{\infty}\frac{a^{n+1}}{n}c_n\psi_n, \tag{A 6}$$

where

$$\psi_n = \frac{\sin n\theta}{r^n} + \frac{\sin n\theta'}{r'^n}. \tag{A 7}$$

This choice for ψ automatically satisfies (A 2), (A 3) and (A 5) for all integers n.

In order to apply the body boundary condition to (A 7), $\sin n\theta'/r'^n$ must be expanded in terms of r and θ. First we note that

$$\operatorname{Im}\frac{1}{(n-1)!}\int_0^\infty k^{n-1}\exp(-k\omega_1)(-1)^n\,\mathrm{d}k = \operatorname{Im}\frac{1}{(n-1)!}\int_0^\infty \frac{t^{n-1}\mathrm{e}^{-t}(-1)^n}{\omega_1^n}\,\mathrm{d}t$$

$$= \operatorname{Im}\frac{\mathrm{e}^{-in\theta'}}{r'^n} = \frac{\sin n\theta'}{r'^n} \tag{A 8}$$

where $\omega_1 = y+b+\mathrm{i}x = -r'\,\mathrm{e}^{-\mathrm{i}\theta'}$. With $\omega_2 = \omega_1 - 2b \equiv y-b+\mathrm{i}x \equiv r\,\mathrm{e}^{\mathrm{i}\theta}$ we thus have

$$\frac{\sin n\theta'}{r'^n} = \mathrm{Im}\frac{1}{(n-1)!}\int_0^\infty (-1)^n k^{n-1}\exp(-k\omega_2)\,\mathrm{e}^{-2kb}\,\mathrm{d}k$$

$$= \mathrm{Im}\frac{1}{(n-1)!}\sum_{m=0}^{\infty}\int_0^\infty k^{n+m-1}(-1)^{n+m}\,\mathrm{e}^{-2kb}\frac{\omega_2^m}{m!}\,\mathrm{d}k$$

$$= \sum_{m=0}^{\infty}\frac{(-1)^{n+m}\,r^m\sin m\theta}{m!}\frac{(n+m+1)!}{(n-1)!\,(2b)^{n+m}}; \tag{A 9}$$

therefore

$$\psi = \frac{a^{n+1}}{n}\sum_{n=1}^{\infty} c_n\left(\frac{\sin n\theta}{r^n} - \sum_{m=1}^{\infty} B_{mn}\frac{n}{m}\frac{r^m}{a^{n+m}}\sin m\theta\right), \tag{A 10}$$

where

$$B_{mn} = \frac{(-1)^{n+m-1}(n+m-1)!\,\lambda^{n+m}}{n!(m-1)!}, \quad \left(\lambda = \frac{a}{2b}\right). \tag{A 11}$$

The boundary condition (A 4) gives

$$U\sin\theta = \sum_{n=1}^{\infty} c_n\left(\sin n\theta + \sum_{m=1}^{\infty} B_{mn}\sin m\theta\right) \tag{A 12}$$

and equating coefficients of $\sin m\theta$ leads to

$$\delta_{1m} = c_m + \sum_{n=1}^{\infty} B_{mn}\,c_n \tag{A 13}$$

Now λ is always less than $\frac{1}{2}$, and if $\lambda = 0$ all the unknown coefficients c_n vanish, except c_1 which is equal to 1, so we expand all the coefficients c_n in powers of λ. Retaining terms up to $O(\lambda^5)$ in (A 13) gives rise to the results

$$\left.\begin{aligned} c_1 &= (1+\lambda^2+\lambda^4)+0(\lambda^6), \quad & c_2 &= -2\lambda^3(1+\lambda^2)+0(\lambda^6),\\ c_3 &= 3\lambda^4+0(\lambda^6), & c_4 &= -4\lambda^5+0(\lambda^6). \end{aligned}\right\} \tag{A 14}$$

The force on the cylinder is given by

$$\left.\begin{matrix} F_x \\ F_y \end{matrix}\right\} = \tfrac{1}{2}a\rho h\int_0^{2\pi} |\nabla\Psi|^2_{r=a}\left\{\begin{matrix}\sin\theta\\ \cos\theta\end{matrix}\right\}\mathrm{d}\theta \tag{A 15}$$

using the same notation as in §3. Some algebra reveals that

$$F_y = -2\rho a h\pi U^2\sum_{n=1}^{\infty} c_n\,c_{n+1}, \tag{A 16}$$

whilst $F_x = 0$, where simplifications are achieved by repeated use of (A 13), showing that, as expected from D'Alembert's paradox, the force in the x-direction vanishes but there is a non-zero force in the y-direction. Use of (A 14) shows that

$$F = -2\pi a h\rho U^2\lambda^3(1+2\lambda^2)+O(\lambda^7), \tag{A 17}$$

which thus represents a suction force.

Appendix B

The cases $M = 0$ and $M = 1$ show that $A_0^j, A_{\pm 1}^j$ are all $O(1)$ as $\kappa a \to 0$. Increasing M to 2 and examining the orders of magnitude of the additional equations shows that $A_{\pm 2}^j$ must be $O(\kappa a)^{-1}$. The matrix equation can then be scaled and reduced to a 4×4 block matrix equation of the form:

$$\begin{bmatrix} I & O & O & A \\ O & I & B & O \\ O & C & I & O \\ D & O & O & I \end{bmatrix} \begin{bmatrix} X_1 \\ X_2 \\ X_3 \\ X_4 \end{bmatrix} = \begin{bmatrix} R_1 \\ R_2 \\ R_3 \\ R_4 \end{bmatrix}, \tag{B 1}$$

where

$$A = \begin{pmatrix} -a & b \\ c & -d \end{pmatrix}, \quad B = \begin{pmatrix} d^* & c^* \\ b^* & a^* \end{pmatrix},$$

$$C = \begin{pmatrix} a & b \\ c & d \end{pmatrix}, \quad D = \begin{pmatrix} -d^* & c^* \\ b^* & -a^* \end{pmatrix},$$

$$a = -4\mathrm{i}\lambda^3, \quad b = -3\lambda^4, \quad c = \lambda^2, \quad d = -\mathrm{i}\lambda^3,$$

$$X_1 = \begin{pmatrix} A_{-2}^1 \kappa a \\ A_{-1}^1 \end{pmatrix}, \quad X_2 = \begin{pmatrix} A_1^1 \\ A_2^1 \kappa a \end{pmatrix},$$

$$X_3 = \begin{pmatrix} A_{-2}^2 \kappa a \\ A_{-1}^2 \end{pmatrix}, \quad X_4 = \begin{pmatrix} A_1^2 \\ A_2^2 \kappa a \end{pmatrix},$$

$$R_1 = R_3 = \begin{pmatrix} 0 \\ \mathrm{i}\, e^{\mathrm{i}\beta} \end{pmatrix}, \quad R_2 = R_4 = \begin{pmatrix} -\mathrm{i}\, e^{-\mathrm{i}\beta} \\ 0 \end{pmatrix}.$$

All the elements of this system are $O(1)$ as $\kappa a \to 0$, smaller terms having been neglected. Solving (B 1), which is straightforward if laborious, leads to expressions for $A_{\pm 1}^j$ which differ from (4.2) in terms of high order in λ. Increasing the truncation size still further would presumably give more accurate formulae for these coefficients in terms of λ and there is no way of telling how accurate our present results are. Comparison with numerical solutions to the exact system of equations shows that they are correct up to at least $O(\lambda^4)$ and results up to this order are given in (4.4).

REFERENCES

Eatock Taylor, R. & Hung, S. M. 1985 Wave drift enhancement effects in multi-column structures. *Appl. Ocean Res.* **7**, 128–137.

Gradshteyn, I. S. & Ryzhik, I. M. 1965 *Tables of Integrals, Series and Products.* Academic.

Kagemoto, H. & Yue, D. K. P. 1986 Interactions among multiple three-dimensional bodies in water waves: an exact algebraic method. *J. Fluid Mech.* **166**, 189–209.

Kim, M.-H. & Yue, D. K. P. 1989 The complete second-order diffraction solution for an axisymmetric body. Part 1. Monochromatic incident waves. *J. Fluid Mech.* **200**, 235–264.

MacCamy, R. C. & Fuchs, R. A. 1954 Wave force on piles: A diffraction theory. *US Army Coastal Engineering Research Center, Tech. Mem.* **69**.

Martin, P. A. 1985 Integral-equation methods for multiple scattering problems. I. Acoustics. *Q. J. Mech. Appl. Maths* **38**, 105–118.

McIver, P. 1987 Mean drift forces on arrays of bodies due to incident long waves. *J. Fluid Mech.* **185**, 469–482.

McIver, P. & Evans, D. V. 1984 Approximation of wave forces on cylinder arrays. *Appl. Ocean Res.* **6**, 101–107.

Mingde, S. & Yu, P. 1987 Shallow water diffraction around multiple large cylinders. *Appl. Ocean Res.* **9**, 31–36.

Molin, B. 1979 Second-order diffraction loads upon three-dimensional bodies. *Appl. Ocean Res.* **1**, 197–202.

Ohkusu, M. 1974 Hydrodynamic forces on multiple cylinders in waves. In *Proc. Intl Symp. on Dynamics of Marine Vehicles and Structures in Waves, London, Paper* 12, pp. 107–112.

Simon, M. J. 1982 Multiple scattering in arrays of axisymmetric wave-energy devices. Part 1. A matrix method using a plane-wave approximation. *J. Fluid Mech.* **120**, 1–25.

Spring, B. H. & Monkmeyer, P. L. 1974 Interaction of plane waves with vertical cylinders. In *Proc. 14th Intl Conf. on Coastal Engineering*, Chap. 107, pp. 1828–1845.

Twersky, V. 1952 Multiple scattering of radiation by an arbitrary configuration of parallel cylinders. *J. Acoust. Soc. Am.* **24**, 42–46.

Záviška, F. 1913 Über die Beugung elektromagnetischer Wellen an parallelen, unendlich langen Kreiszylindern. *Annln. Phys.* **40**, 1023–1056.